Combined design and control optimization of heat pumps in residential buildings

Phani Arvind Vadali, Dr. Moncef Krarti

Civil, Environmental, and Architectural Engineering,

University of Colorado, Boulder

Abstract

Electrification of buildings through deployment of heat pumps requires innovative design and control strategies to reduce their energy demands on the grid. Instead of the sequential approach of optimizing the design specifications and control strategies, this paper considers the benefits of the combined and simultaneous optimization of design capacities and control settings for heat pumps when specified for US residential buildings. A Genetic Algorithm optimizer is used to simultaneously adjust the main and supplementary coil capacities for the heat pump as well as the indoor temperature setpoints to minimize annual heating and cooling energy needs as well as occupant thermal discomfort levels. In comparison to design and control baselines, it is found that simultaneous optimization can achieve 21% and 7% reductions in heating and cooling annual energy consumption for the cases of variable speed and single speed heat pumps. Moreover, the analysis results indicate that these reductions are nearly double the savings obtained when design only and control only based optimizations are considered. The presented combined design and control optimization approach could potentially provide an effective paradigm shift in specifying heat pump systems for residential buildings.

Keywords: Heat Pumps, Residential Buildings, Optimization, Genetic Algorithms, Design, Control

Nomenclature

Abbreviations:

AHRI - Air-Conditioning, Heating, and Refrigeration Institute

ASHRAE – American Society of Heating, Refrigeration and Air-conditioning Engineers

AZ – Arizona

CA - California

CHP – Combined Heat and Power

COP – Coefficient of Performance

DX – Direct Expansion

EIR – Energy Input Ratio

GA - Genetic Algorithm

HVAC – Heating, Ventilation, and Air-Conditioning

MILP – Mixed Integer Linear Programming

OSB – Oriented Strand Board

PMV – Predicted Mean Vote

PPD – Predicted Percentage Dissatisfied

PSO – Particle Swarm Optimizer

PV – Photovoltaic

RC – Resistor Capacitor

RTF – Run Time Fraction

PLF – Part Load Fraction

PLR – Part Load Ratio

TES – Thermal Energy Storage

TSE – Total Site Energy

Variables

a – Exponent coefficient for thermal discomfort comfort penalty function [-]

cfm – cubic feet per minute [m^3/s (ft^3/min)]

EIR_r – Energy Input Ratio at rated conditions [-]

$F_D(X)$ – Annual discomfort penalty [-]

$F(X)$ – Optimization objectives vector [-]

f_C^T – Capacity multiplier as a function of indoor and outdoor temperature [-]

f_C^V – Capacity multiplier as a function of fraction of flow rate [-]

f_{EIR}^T – EIR multiplier as a function of indoor and outdoor temperature [-]

f_{EIR}^V – EIR multiplier as a function of fraction of flow rate [-]

$\dot{P}$ - Power consumed by the compressor [W (Btu/hr)]

$P(\boldsymbol{x}, t)$ – Hourly discomfort penalty [-]

$\dot{Q}_C$ – Actual cooling capacity [$W(Btu/hr)$]

$\dot{Q}_{r,C}$ – Cooling capacity at rated conditions [$W(Btu/hr)$]

$T_{db,in}^c$ – Dry bulb temperature of air entering the condenser [$°C$($°F$)]

T_{disc} – Number of discomfort hours [-]

$T_{wb,in}^e$ – Wet bulb temperature of air entering the evaporator [$°C$($°F$)]

$\dot{V}_r$ – Volume flow rate of air at rated conditions [m^3/s (ft^3/min)]

$\dot{V}$ – Actual volume flow rate of air [m^3/s (ft^3/min)]

W – Penalty factor to define the well function as a discomfort objective [-]

x – Vector containing all inputs required to calculate PMV

X – Vector representing a single individual of the GA

λ – Penalty weighting factor for thermal discomfort [-]

1. Background

Residential buildings account for 22% of the total energy consumed in the United States [1]. Space heating alone is responsible for 42% of the energy consumed by the residential sector followed by water heating and space cooling accounting for 18% and 9% respectively. Electricity use, accounting for a significant portion of the energy needs of US building, is expected to increase in the forthcoming years due to various federal and state decarbonization programs and initiatives [2]. Therefore, developing efficiently designed and controlled heating and cooling systems will be crucial to lower electricity demands for buildings.

Studies show that optimal design and operation of building energy systems has been extensively considered for a wide range of applications. Barber and Krarti [3] provide a comprehensive review of various design and control optimization methods that have been applied to building energy systems including heat pumps and PV arrays as well as building envelope elements such as thermal insulation and glazing systems. However, optimization of design and control of building energy systems is typically done in a sequential manner. First, the design of the energy system is optimized based on a generic unoptimized control strategy after which the control scheme is then optimized. The combined and simultaneous optimization of both design and control of building energy systems is a rather new but promising area of research. The primary goal in combined design and control optimization is to identify simultaneously and interactively the best design specifications and operation strategies to maximize/minimize desired objectives with a set of constraints. The vast majority of reported studies address optimizing either the design or the control schemes individually rather than simultaneously [3]. The limited available studies that combine design and control optimization have indicated significant improvements in the performance for building energy systems compared to those obtained from individual optimization [4].

However, the interactive nature of design and control parameters complicates the process of combined optimization. A common approach to determine the best design and control solutions simultaneously is to perform sequential optimization. Sequential optimization is a two-step process wherein design specifications of energy system operating using a pre-defined control scheme are first optimized. Subsequently, this process is then repeated several times for different control settings until optimal design-control solutions are identified. This nested optimization scheme can be computationally expensive [5], especially when the analysis is carried out using whole building energy simulation tools such as Energy Plus [6] and TRNSYS [7]. However, most of the building energy simulation tools have limited abilities to implement complex control schemes and often rely only on rule-based control strategies [8]. Thus, other tools such as Spawn [9] and BCVTB [10], are often considered to implement advanced control strategies. Another challenge for achieving combined design and control optimization is the nature of the objective function. Commonly used objective functions including minimizing annual energy cost, annual energy use, and carbon emissions often yield non-convex, and non-differentiable objective functions making it difficult to identify global optimum solutions [11].

To address the complexities of combined design and control optimization of building energy systems, researchers have used a variety of techniques and approaches. Pattteuw and Helsen [4] as well as Ashouri et al [12] used a single Resistor – Capacitor (RC) model for the building and linear models for the energy systems to optimize their selection, sizing, and operation for a grid consisting of up to 1 million buildings [4] as well as for a single a commercial building in Zurich [12]. The advantage of using linear

models is that the optimization problem can be solved using Mixed Integer Linear Programming (MILP) which guarantees a globally optimum solution [1],[4]. The number of well-established MILP solvers also contributes to its increased application in solving design and control optimization problems for building energy systems [13]. In addition to MILP based methods, metaheuristic methods such as Genetic Algorithms (GA) [14] have been used to solve optimization problems with non-convex objective functions. The most widely used GA approach is the Non-dominated Sorting Algorithm (NSGAII) developed by Deb [15]. Since metaheuristic methods do not depend on the gradient, they could be better equipped to handle complex objective functions. However, previous reported analyses have indicated that these methods do not necessarily achieve global optimal solutions. Some studies have used the nested design and control optimization frameworks to combine GA and MILP based methods to utilize the benefits of each approach.

Indeed, Evins [5] used a MILP framework for optimizing the operation of several energy conversion and storage systems including heat pumps, PV arrays, absorption chillers, batteries, as well as hot and chilled water energy storage tanks when deployed to office buildings. The control optimization was nested using GA-based optimization approach to select the capacities the energy systems as well as the specifications of building envelope elements such as the size of windows and the thickness of insulation layers. Using equivalent annual costs and carbon emissions as the optimization objective functions, 20 potential solutions were identified, each of which had a payback period of less than $20\ years$. Similarly, Urbanucci et al [13] developed a nested optimization framework using an MILP based optimizer for the control and a GA based optimizer for the design specifications. This nested optimization framework was applied to a combined heat and power (CHP) plant augmented by an auxiliary boiler and a thermal energy storage (TES) system to meet the energy demands of a secondary school. The analysis results indicate that the combined design and control optimization framework allows for 70% of the school's energy demand to be met by the CHP while the remainder of the load can be shared between the TES, boiler, and the grid.

By comparing the effectiveness of the two different optimization techniques, Fazlollahi et al [16] identified that though GA based techniques can handle multiple objectives better than those using MILP, they are computationally more expensive. To reduce complexity, Bahlawan et al [11] considered surrogate modeling of the objective function using a radial basis function coupled with dynamic programming to perform a combined design and control optimization of a power plant serving a university campus. Their analysis found that the surrogate modeling approach is 78% faster than a Particle Swarm Optimizer (PSO).

A vast majority of the reported applications for the combined design and control optimization have been related to generation and storage systems for power plants with only very limited studies considered applications to buildings. Moreover, the energy demand estimations for the reported studies are based on various sources including predictions from whole building energy simulation tools [14], data from smart meters and utilities [17] and other standardized sources [18]. These energy demands are considered as constraints for the optimization framework utilized by most reported studies thereby avoiding any need for predicting the energy requirements during the optimization process. Some limited studies have used a lumped modeling approach wherein all energy conversion devices, storage devices, and consumption devices are modeled as one group to simplify the optimization problem. Ashouri et al [12] used the energy hub to lump devices together and simplify the setup of the combined optimization problem. Beck et al [17] and Evins [5] also used the simplified lumped modeling framework of the energy hub combined with linear programming to carry out combined design and control optimizations.

Several objective functions have been considered for the optimal design and control of energy systems including indicators of economic, environmental, and social impacts. The equivalent annual cost (EAC), defined as the annualized cost of investment and operation of the energy systems, is the most widely used economic metric in the reported literature. Other economic objective functions include global cost for

space conditioning [14] and total cost of ownership [17]. A few studies have also considered environmental based indicators as objective functions for the optimization analysis. For instance, Mehleri et al [19] utilized the carbon content of the purchased electricity and natural gas and the carbon tax rate to quantify the cost of carbon emissions. They used this metric along with the total annualized cost to determine the optimal size, operation, and pipeline network of a microgrid supplying energy to a Greek residential neighborhood. Their optimization analysis found that using a CHP system and a PV system can achieve up to 89.7% savings in annualized cost when compared to the conventional case of purchasing energy needs from the grid. Social objective functions including the percentage of energy generated by PV exported back to the grid have also been considered for design and control optimization of energy systems [18].

Moreover, some reported studies have considered occupant discomfort as part of the optimization framework but usually in the form of a constraint to ensure the indoor temperature is within the comfortable range. No reported study has explicitly included occupant thermal comfort indicators as part of the combined design and control optimization process. Ascione et al [14] did consider Predicted Percentage of Dissatisfied (PPD) as part of their objective function in addition to operating costs, to optimize the design and control of the HVAC system of a residential building but, their design optimization is only based on selection existing systems without their sizing. Therefore, there is a need to investigate how occupant thermal discomfort can be accounted for in a combined design and control optimization framework using more advanced models.

In summary, the review of the reported literature indicates that no analysis has been carried out for optimally integrating the design and the operation of heat pumps when deployed in new or existing residential buildings. This paper provides the first analysis of simultaneously optimizing the design specifications and operating settings for heat pumps. Specifically, the study describes a new analysis approach that investigates the benefits of optimally combining the design and control of heat pumps for US residential buildings when compared to those achieved from the design only and control only optimizations. First, a brief description of the prototypical US residential building considered in the study is provided. Then, the general analysis approach is outlined including the optimization objective function and related constraints. A set of optimized design and control settings for the baseline building model are initially identified to conduct fair comparative assessments with design-only, control-only, and combined design and control optimization results. Finally, the impacts on both building energy efficiency and indoor thermal comfort of various heat pump design and operation parameters are evaluated through a series of sensitivity analyses.

2. Analysis Approach

The analysis approach considered throughout the study to investigate the benefits for integrating design and control optimizations is illustrated in Figure 1. The combined optimization includes four key components: building energy model, design and control parameters, objective functions, and constraints.

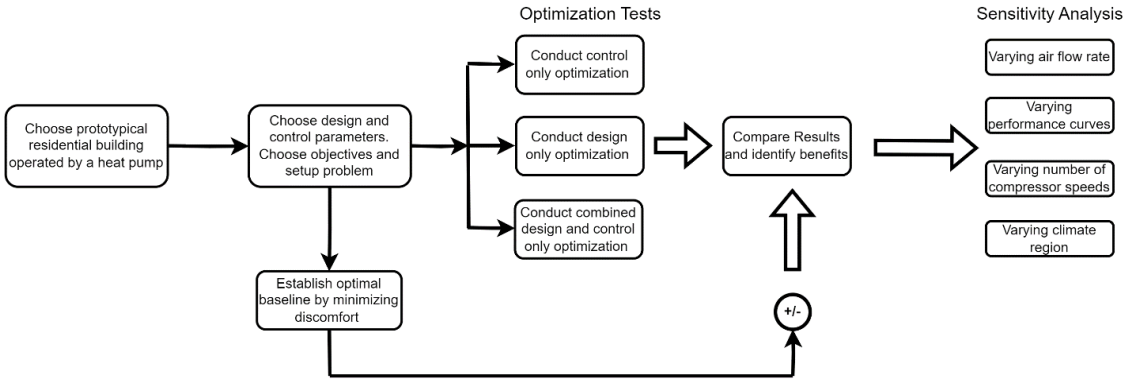

Figure 1 Flowchart of analysis approach.

2.1 Building Energy Model

For this study, a prototypical energy model for an electrified US house is considered [20]. The main characteristics of the house are summarized in Table 1. An air-to-air heat pump is used to maintain acceptable indoor air temperature within conditioned living spaces. The heat pump has a single-speed compressor with direct expansion heating/cooling coils and a supplementary electric heating coil. The heating and cooling capacities of the heat pump are provided in Table 2.

Table 1: Main characteristics for the prototypical electrified residential building

Total Floor Area	$331\ m^2 (3566\ ft^2)$
Exterior Wall Construction	Synthetic Stucco / Sheathing/ $\frac{7}{16} in.$ OSB / Wall Console Layer / $0.5\ in.$ Drywall
Foundation	Concrete slab-on-grade floor
Exterior Roof Construction	Asphalt Shingles / $0.5\ in.$ OSB
Window Construction	Standard glass with U factor of $1.7\ W/m^2K$ and SHGC 0.33 with interior blinds
Window-To-Wall Ratio	14.12% (2 windows on each wall)
Shading	East facing windows only with depth of $1.52\ cm$ $(0.6\ in)$
Number Of Occupants	3
Electric Equipment	Dishwasher $(65.7\ W)$, Refrigerator $(91.05\ W)$, Clothes Washer $(28.47\ W)$, Clothes Dryer $(213.06\ W)$, Electric Range $(248.1\ W)$, Misc. electric equipment $(567.46\ W)$, Misc. Plug loads $(1.54\ W/m^2)$
Lighting Power Density	Hardwired $(1.05\ W/m^2)$, Plug-in $(0.47\ W/m^2)$
Schedules	All schedules based on BA Housing Simulation Protocols [21]
Thermal Zones	Living zone and unconditioned attic zone

Temperature Setpoint	Heating setpoint – $22.222°C$ $(72°F)$ Cooling Setpoint - $23.888°C$ $(75°F)$

Table 2: Heating and Cooling Capacities for the Baseline Air Source Heat Pump

	Coil Type	**Supply Air Flow Rate $[m^3/s]$**	**COP**	**Nominal Capacity $[kW]$**
Cooling	Single Speed DX cooling coil	0.364	4.068	5.75
Heating	Single Speed DX heating coil	0.364	3.69	5.75
Supplementary heating	Electric heating coil	0.364	-	6.48

2.2 Design and Control Parameters

To assess the benefits of integrated design and control optimization of the heat pump two parameters of each category are considered:

1. Design Parameters: Heating and cooling capacities of the heat pump
2. Control Parameters: Heating and cooling temperature setpoints

The temperature setpoints are "soft" control parameters rather than actual control actions set for the heat pump. That is, these parameters do not set when the heat pump switches on and off but rather they rely on the capabilities of heat pump, modeled using the whole building energy simulation tool Energy Plus [8], to maintain the desired indoor thermal comfort. Specifically, Energy Plus does not control the heat pump to maintain any desired temperature setpoint but instead estimates the thermal load required to achieve this setpoint. If the capacity of the heat pump is greater than the estimated load, the temperature setpoint is assumed to be met [22].

Furthermore, Energy Plus models a heat pump as a unitary air to air heat pump that has a main coil that does both heating and cooling through the direct expansion of a refrigerant and an additional electric coil for any supplementary heating needs [22]. Therefore, the design parameters of the heat pump refer to the capacities of both the main and supplementary coils.

The ranges of both design and control parameters along with the incremental steps used in the study are described in Table 3. The coil size of the heat pump is limited by the amount of air flowing through the system. Rated coil capacities cannot be achieved without allowing the air flow rates to be delivered at their rated levels by the system. For the optimization of coil size with fixed flow rate, the maximum achievable capacity was determined to be twice the original size. Hence, the range of sizing factors was chosen to be in between 0.8 and 2. Later in the study, the effects of changing air flow rate on the optimization results are investigated. The potential options for heating temperature setpoint to be considered in the optimization analysis are determined by evaluating which range has the highest chance of minimizing thermal discomfort levels. The cooling setpoint range is selected as a function of the heating setpoint and varies from a minimum value equal to the heating setpoint to a maximum value of being $4°C$ above the heating setpoint.

Table 3 Ranges of design and control parameters.

	Main Coil Capacity	Supplementary Coil Capacity	Heating Setpoint	Cooling Setpoint
Minimum	4.60 kW	5.19 kW	21°C	=(Heating Setpoint)
Maximum	11.50 kW	12.96 kW	26°C	=(Heating Setpoint + 4.0°C)
Increment	0.29 kW	0.32 kW	0.5°C	0.5°C

2.3 Optimization Objective Functions

Several metrics can be used to quantify the performance of building energy systems including operational costs, life cycle costs, carbon emissions, and thermal comfort levels. This study considers annual energy consumption and thermal comfort performance of building as the main metrics for the optimization analysis. The annual energy consumption is estimated as the total site energy (TSE) consumed by the building and encompasses all energy end-uses including heating, ventilation, and air conditioning (HVAC), lighting energy, and appliances. The thermal comfort performance of the building is estimated using the Predicted Mean Vote (PMV) metric as defined by ASHRAE standard 55 [23] ranging from -3 (very cold) to $+3$ (very hot). An indoor environment is considered comfortable if its PMV is between -0.5 and $+0.5$ which corresponds to less than 10% of the occupants being dissatisfied with the indoor thermal comfort level. The value of PMV depends on six factors namely, air temperature, relative humidity, relative air speed, mean radiant temperature, clothing level, and activity level [23].

Table 4 lists the values of parameters used to determine the PMV within the house. Three parameters are pre-determined including air velocity, occupant activity level, and clothing level while the remaining three parameters namely the indoor temperature, relative humidity, and the mean radiant temperature are estimated by the simulation engine during each time step. The values for the pre-determined parameters are based on nominal values provided by ASHRAE 55 [23]. Figure 2 shows the distribution of air humidity ratios and operative temperatures for the baseline case of the house and indicates thermal comfort regions for both summer and winter seasons. The main characteristics are listed in Table 1 and the design specifications outlined in Table 2. The operation settings of the baseline house energy model including indoor air velocity, indoor temperature settings, as well as activity and clothing levels for occupants are summarized in Table 4. For this study, the house is considered to be uncomfortable during a given time step (i.e., typically one hour), only if its thermal conditions are estimated to be outside both the summer and winter comfort regions as indicated in red by Figure 2.

Table 4 Values of main parameters used to estimate Predicted Mean Vote (PMV) for the residential building

	Parameter	Value
Constant at all times for all the cases tested	Constant air velocity	0.15 m/s
	Activity level	117.28 $W/per\ person$ = 1.12 met
	Clothing Level	0.5 clo (summer) – 1 clo (winter)
	Heating Setpoint	22.2°C (72°F)

Calculated at every time step for each case	Cooling Setpoint	$23.9°C$ $(75°C)$
	Mean Radiant Temperature	Zone Averaged value
	No. of discomfort hours i.e., hours outside boundaries of comfort region (in red)	596 *hours*

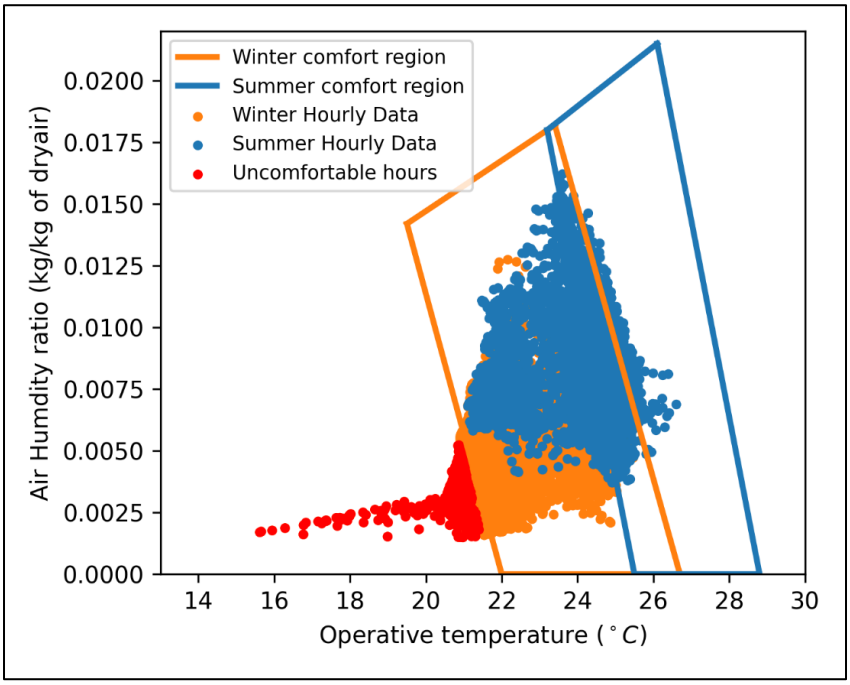

Figure 2 Hourly indoor conditions for the chosen prototypical residential building model for one year where the red dots represent hours outside thermal comfort zones during both summer and winter seasons.

Thus, the indoor environment is considered thermally comfortable when the PMV value is within the range of -0.5 and $+0.5$. This thermal comfort constraint is included in the optimization objective function using a penalty function. For this study, an hourly penalty function, $P(\boldsymbol{x}, t)$, is considered as a function of time t (expressed in hours), and vector $\boldsymbol{x}$ representing all the parameters required to calculate PMV as specified in Table 4. The annual penalty function is calculated as the sum of all values of the hourly penalty functions as expressed by Eq. (1):

$$F_D(X) = \sum_{t=1}^{8760} P(\boldsymbol{x}, t) \tag{1}$$

In this study, three variations are considered for the hourly penalty functions including:

1. Residuals of PMV relative to thermal comfort minimal and maximal thresholds:

$$P(X,t) = \begin{cases} \lambda(\max\{0, PMV(X,t) - 0.5\})^a & PMV > 0.5 \\ 0 & -0.5 < PMV < +0.5 \\ \lambda\,(\min\{0, PMV(X,t) + 0.5\})^a & PMV < -0.5 \end{cases} \tag{2}$$

Where $PMV(X,t)$ is the value of PMV at every hour, and λ and a are constants that that can be set before the optimization is carried out. The penalty function presents the absolute sum of residuals for $a = 1$ and squared sum of residuals for $a = 2$.

2. Absolute Sum of PMV Squares:

$$P(\boldsymbol{x},t) = \left(PMV(\boldsymbol{x},t)\right)^2 \tag{3}$$

3. Well function for the PMV to be within acceptable range:

$$P(\boldsymbol{x},t) = \begin{cases} W & PMV > 0.5 \\ 0 & -0.5 \leq PMV \leq +0.5 \\ W & PMV < -0.5 \end{cases} \tag{4}$$

Where W is the value of the penalty. When the value of W is equal to 1, the well function is essentially a count of the total number of hours wherein the PMV value is outside the thermal comfort acceptable range, that is, the total number of thermal discomfort hours.

Figure 3 shows the variations with PMV values for the three penalty functions defined above and considered in this study.

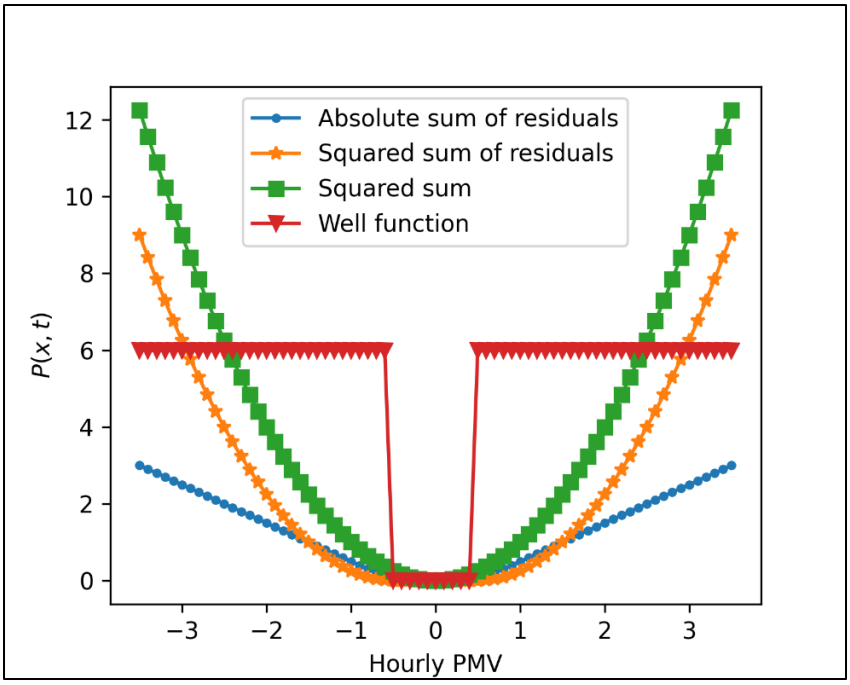

Figure 3 Penalty functions specific to define indoor thermal comfort.

Using the two objectives defined in the current section including *TSE* and F_D, a bi-objective optimization problem can be setup as follows,

$$\min F(X) = \left(TSE, F_D(X)\right)^T \tag{5}$$

Where X is the vector of parameters for both design (i.e., capacities for the main and supplementary coils) and control (i.e., heating and cooling temperature setpoints).

Subject to:

$$T_{disc} < 1200\ hour \tag{6}$$

Where T_{disc} is the total number of discomfort hours in the whole year.

The framework establishes a bi-objective optimization problem which means that the optimizer tries to simultaneously minimize both objective functions (i.e., *TSE* and F_D). In general, solving bi-objective optimization is done by combining both objective functions into one by assigning weights to each function. In this study instead of formulating a single objective function, the optimizer is allowed to choose and vary the weights and solve the problem. Thereby, based on the weight, a set of solutions is obtained forming a Pareto frontier to simultaneously minimize both objective functions.

2.4 Baseline Design and Control Settings

To compare the results of the combined design and control optimization using the bi-objective framework, a baseline is first established. A typical method for defining a baseline is to set the design and control specifications of the heat pump using an established standard [20]. However, this approach results in high discomfort level for the occupants of the house during several hours ($i.e., 596\ hours$) as shown in Table 4. Therefore, the design and control parameters specific to the heat pump for the baseline case of the residential building need be adjusted to ensure consistent indoor thermal comfort and to ultimately conduct fair comparative analyses when other design and/or control settings are considered. The new design and control parameters of the baseline heat pump system are identified by minimizing the discomfort level of the house, irrespective of the required energy consumption.

3. Analysis Results

The optimization analyses are carried out using a Genetic Algorithm (GA) technique combined with a whole building energy simulation engine, EnergyPlus, considered a state-of-art energy analysis tool [24]. The optimizer is based on the Non-dominated Sorting Genetic Algorithm II (NSGAII) [15] with the search domain specified by user-defined discrete options for various design and control parameters. Table 3 lists the sets of design and control parameters considered in the optimization analyses including 169 options for the heat pump capacities and 99 options for the control parameters. The ranges of each of the variables have been identified based on a set of parametric analyses conducted to balance the required simulation time and the desired indoor thermal comfort levels. The GA is set to have an initial population of 10, a crossover and mutation rate of 100% and 20%, respectively and a maximum number of generations of 50. The selected GA settings are selected based on a series of parametric analyses to minimize the simulation time while maintaining acceptable accuracy levels to reach optimal solutions.

To identify the benefits of integrated design and control optimization, first the design and control parameters for the baseline heat pump are adjusted to ensure that acceptable indoor thermal comfort levels are achieved. Then, design only, control only, as well as combined design and control optimizations are conducted using the objective function of Eq. (5). The results of these analyses are discussed in the following sections.

3.1. Optimized Baseline Settings

The baseline model for the residential building is used in this study as a reference to compare the performance of optimal design and/or control configurations. The initial design and control parameters of the prototypical residential building model defined in Table 1 and Table 2 are adjusted to minimize the indoor thermal discomfort levels. These adjustments are made to ensure fair comparisons with the performance metrics achieved by the optimal design and/or control cases set to minimize the building's annual total site energy consumption as well as the indoor thermal discomfort level. Figure 4 shows a histogram plot of the total site energy of all potential baseline heat pump capacities and temperature settings obtained as solutions when indoor thermal discomfort levels are minimized using only $F_D(X)$, defined by Eq. (1), as the objective function.

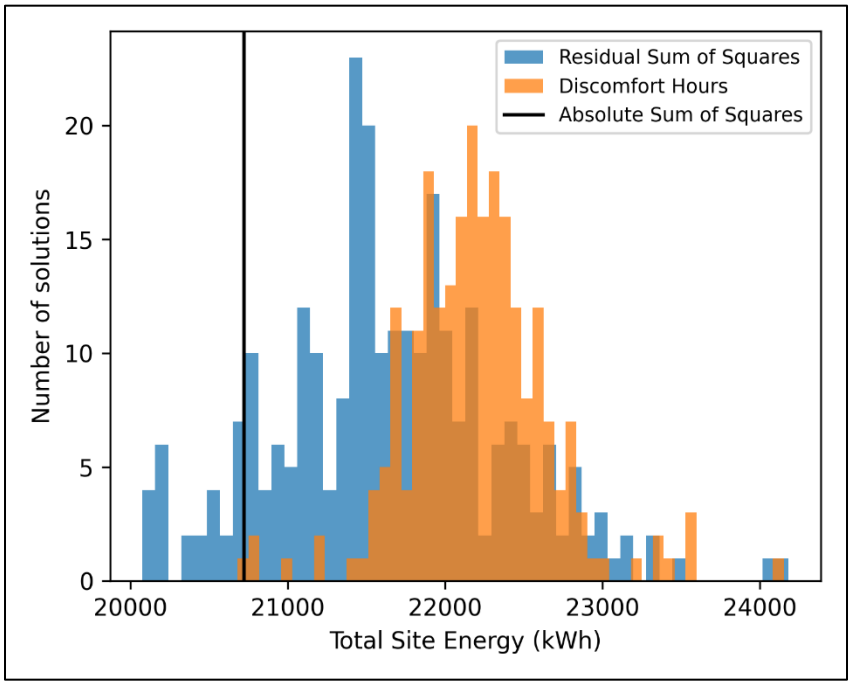

Figure 4 Histogram plot of total site energy of all optimal solutions obtained when minimizing discomfort using various penalty functions.

Each of the potential solutions shown in the histogram plot has 0 discomfort hours. As indicated by the results of Figure 4, the optimal solutions obtained using the residual sum of squares as the objective function yield baseline configurations with the least total site energy. Therefore, the indoor thermal discomfort penalty using residual sum of squares is considered for the remaining optimization analyses carried out for this study. The baseline heat pump capacities and temperature settings, adjusted to ensure indoor thermal comfort is maintained while minimizing building energy consumption, are listed in Table 5.

Table 5 Heat pump capacities and heating/cooling temperature settings for the baseline building energy model.

Type of Heat Pump	Single - speed
Main Coil Capacity	11.5 kW (39260 Btu/hr)
Supplementary Electric Heating Coil Capacity	10.7 kW (36476 Btu/hr)
Air Flow Rate	0.364 m^3/s (77.12 cfm)

Heating Setpoint Temperature	$23.5°C$ $(74.3°F)$
Cooling Setpoint Temperature	$25.3°C$ $(77.5°F)$
Annual Total Site Energy	$20075\ kWh$ $(68500\ kBtu)$
Number of discomfort hours	0

3.2. Optimization Analysis Results

In this section, the design and/or control optimization results are discussed and compared to those obtained for the adjusted baseline case using two performance indicators including annual energy consumption and indoor thermal comfort level.

3.2.1. Control Only Optimization

Control only optimization involves determining the best heating and cooling temperature setpoints that minimize both annual energy consumption and indoor thermal discomfort for the residential building. To ensure practical solutions, the cooling temperature setpoint is set to be higher than the heating temperature setpoint by an increment varying from $0°C$ to $4°C$. The main and supplementary coil capacities are adjusted by the same sizing factor relative to the capacities listed in Table 2.

Figure 5 shows the Pareto optimal set of solutions for heating and cooling setpoint temperatures to minimize total site energy as well as indoor discomfort level for three sets of heat pump capacities. Irrespective of the sizing factor considered for the heat pump, the optimal Pareto curves of Figure 5 indicate that the number of discomfort hours can decrease only with a decreasing energy savings. For any sizing factor, the number of discomfort levels reach an asymptotic value after which no further improvement of indoor thermal comfort can be achieved even with high energy consumption. This result can be explained by the fact that while the number of discomfort hours are dependent significantly on the temperature setpoint, the ability of the system to maintain the desired thermal comfort level is highly dependent on the heat pump capacity. As coil capacity increases, the ability of the heat pump to maintain indoor thermal comfort improves until the number of discomfort hours is eliminated as indicated for the case of point C with a sizing factor of 1.5. For this sizing factor, the total site energy is higher by 0.74% relative to the adjusted baseline as indicated by point C in Figure 5. When the sizing factor is 1.0, the energy savings can be higher than 7.2% as noted by point B with an acceptable thermal comfort level. This result is consistent with the finding of a reduction of 7% in energy demand of a heat pump operated using an optimized control strategy based on an experimental evaluation [25]. For a sizing factor of 0.75, the potential energy savings can reach 8.1% as noted by point A at the expense of higher discomfort hours as reported by other studies [26-27].

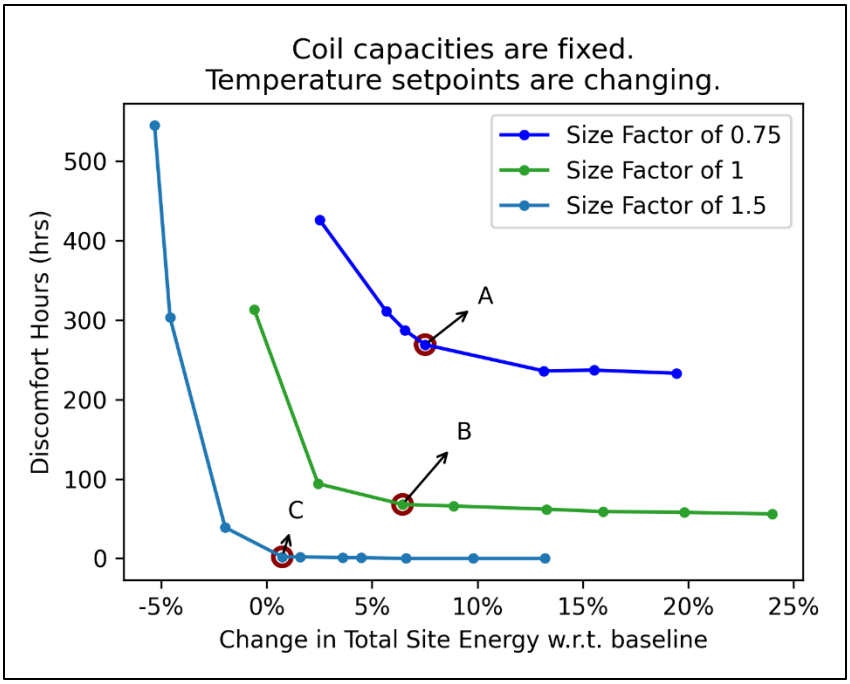

Figure 5 Pareto fronts of solutions obtained by optimizing heating/cooling temperature setpoints showing annual site energy use as a function of discomfort hours for three different heat pump capacities.

3.2.2. *Design Only Optimization*

For the case of design only optimization, the GA optimizer identifies the best capacities for the main and supplementary coils of the heat pump to minimize both annual energy consumption and indoor thermal discomfort hours while keeping the heating/cooling setpoints unchanged. Figure 6 illustrates the design optimization results for three different temperature setpoint options showing the Pareto fronts showing the change in annual site energy use relative to the adjusted baseline and the number of indoor thermal discomfort hours.

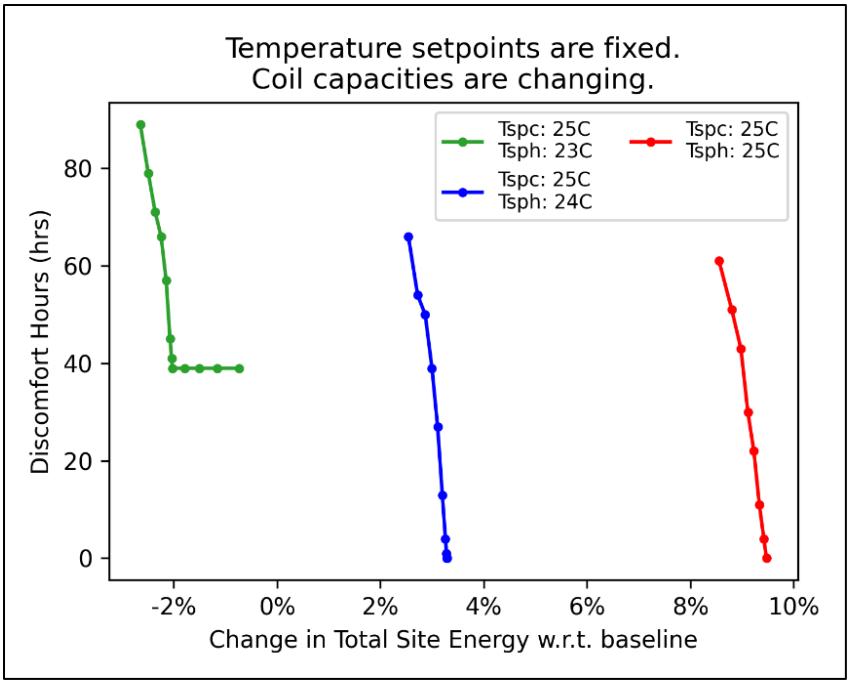

Figure 6 Pareto fronts of solutions obtained by optimizing heat pump capacities showing annual site energy use as a function of discomfort hours for three temperature setpoint combinations.

Figure 6 indicates that while the heat pump capacities significantly affect the indoor discomfort levels, their effects on energy consumption are rather minimal. Specifically, low sizing factors result in higher discomfort hours as noted by other studies [26-27]. However, the selection of temperature setpoints can affect significantly the thermal discomfort level within the house. As indicated by the green curve, when the heating and cooling setpoints are $23°C$ and $25°C$ respectively, an asymptotic point is reached wherein any change in coil capacities cannot further decrease the discomfort hours. For the remaining two setpoint options, the discomfort hours are eliminated (i.e., become 0) after thresholds in heat pump capacities have been reached. As expected, a higher heating setpoint leads to higher energy consumption and therefore lower energy savings in comparison to the adjusted baseline.

3.2.3. *Combined Design and Control Optimization*

Figure 7 shows the Pareto curve for all the solutions obtained when combined optimization of design and control parameters is carried out to minimize both annual site energy use and indoor thermal discomfort level. Like the results obtained when optimizing for the design only or the control only, the combined optimization indicates that higher energy savings can be achieved at the expense of higher discomfort hours. Figure 7 shows two combined design-control optimal solutions A and B as specified in Table 6 with different levels of energy efficiency and thermal comfort. As indicated in Table 6, solution A offers a greater reduction in energy consumption with a higher number of discomfort hours in comparison to those achieved by solution B. The two solutions differ only slightly as they have the same design capacities (i.e., with sizing factors of 1.8 for main coils and 1.5 for supplementary coil) and the same cooling temperature setpoint (i.e., $26°C$) but slightly different heating setpoint (i.e., $22.5°C$ for solution A and $23.0°C$ for solution B). This slight change, however, results in significant reduction in energy performance with HVAC energy savings of 12.3% for A and 7.2% for B. A cost benefit analysis that accounts for both prices of both energy consumption and indoor thermal discomfort could facilitate the selection of the best option between solutions A and B.

Table 6 Specifications and performance indicators for two optimal solutions obtained from integrated design and control optimization.

Optimal Solution	Main Coil Sizing Factor	Supplementary Coil sizing factor	Heating Setpoint	Cooling Setpoint	Reduction in total site energy w.r.t. baseline	Reduction in HVAC energy use w.r.t. baseline	Discomfort Hours
A	1.8	1.5	$22.5°C$	$26°C$	-5.7%	-12.3%	304
B	1.8	1.5	$23°C$	$26°C$	-3.3%	-7.2%	39

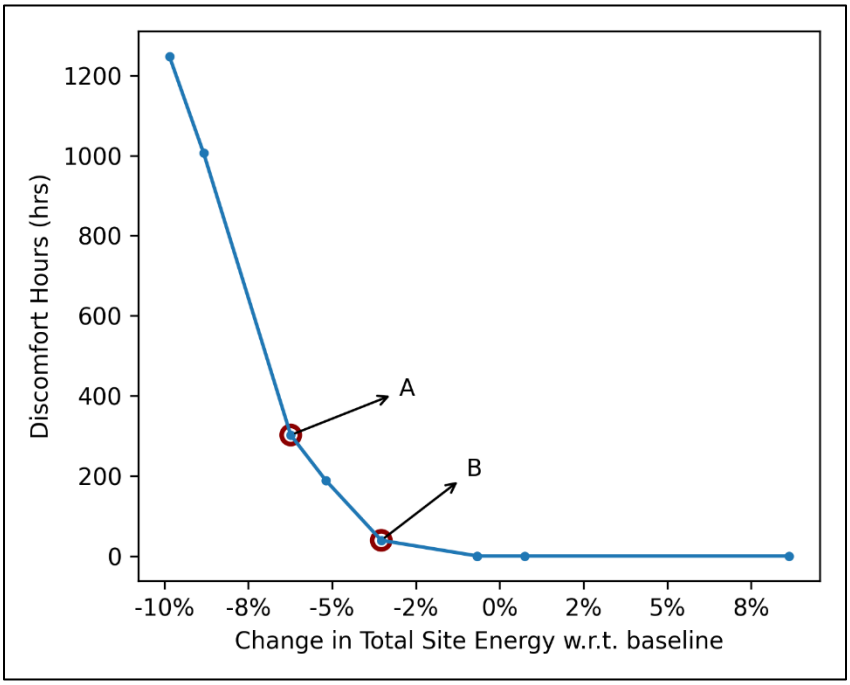

Figure 7 Pareto front of solutions obtained by optimizing both design and control parameters showing annual site energy use as a function of discomfort hours.

3.3. Comparison of Optimal Design and Control Specifications

As indicated by the results of various optimization analyses, there are several potential solutions depending on the considered objective function as well as the desired performance indicators. In general, higher energy savings can be achieved with the compromise of higher indoor thermal discomfort levels and vice versa. For instance, in the case of control only optimization, a system sizing factor of 0.75 (i.e., having a three-fourth the coil capacities listed in Table 5 for the adjusted baseline case) results in a minimum of 200 discomfort hour whereas the same heat pump with twice the heating/cooling coil capacities can eliminate any thermal discomfort level throughout the year in addition to providing some annual energy savings. Similarly, in the case of design only optimization, a heat pump set at a heating setpoint of $23°C$

achieves 2% annual energy savings for the optimal main and supplementary coil capacities with 40 hours of thermal discomfort whereas the same heat pump with a higher heating setpoint of $25°C$ results in more energy consumption than the adjusted baseline but without any thermal discomfort hour throughout the year. These cases illustrate the importance of integrating both design and control parameters together when optimizing energy consumption since considering design only or control only optimization may not achieve the highest energy savings without significantly affecting the thermal discomfort levels. Table 7 compares the reductions in total site energy and HVAC energy use as well as the thermal discomfort hours achieved by the best configurations specific to design only, control only, and combined design/control optimization cases.

Table 7 Comparison of system specifications and performance indicators for the three optimization studies for three levels of discomfort.

	Main Coil Size		**Supplementary Coil Size**		**Heating Setpoint**		**Cooling Setpoint**		**Reduction in Total Site Energy w.r.t. baseline**	**Reduction in HVAC energy use w.r.t. baseline**	**Discomfort Hours**
	Base	Opt	Base	Opt	Base	Opt	Base	Opt			
Control Only	2.0	1.5	1.65	1.5	$23°C$	$23.5°C$	$25.3°C$	$26°C$	$+0.74\%$	-0.31%	2
	2.0	1.5	1.65	1.5	$23°C$	$23°C$	$25.3°C$	$26°C$	-1.96%	-5.3%	39
	2.0	1.5	1.65	1.5	$23°C$	$22.5°C$	$25.3°C$	$26°C$	-4.5%	-10.8%	303
Design Only	2.0	2.0	1.65	1.8	$24°C$	$22.5°C$	$25.3°C$	$25°C$	$+3.3\%$	$+6.8\%$	0
	2.0	2.0	1.65	2.0	$23.5°C$	$23°C$	$25.3°C$	$25°C$	-2.0%	-4.4%	39
	2.0	2.0	1.65	1.3	$23.5°C$	$22.5°C$	$25.3°C$	$25°C$	-4.5%	-9.7%	302
Combined Design and Control	2.0	1.8	1.65	1.7	$23.5°C$	$23°C$	$25.3°C$	$26°C$	-0.66%	-1.7%	0
	2.0	1.8	1.65	1.5	$23.5°C$	$23°C$	$25.3°C$	$26°C$	-3.3%	-7.2%	39
	2.0	2.0	1.65	1.8	$23.5°C$	$22.5°C$	$25.3°C$	$26°C$	-6.23%	-12.9%	302

When the threshold for the thermal discomfort level is set to $40\ hours$ during one year, Table 7 indicates that the best case solution for combined design and control optimization can achieve 3.3% savings in total site energy and 7% savings in HVAC energy use. Control only optimization achieves the best savings when both coil capacities are assumed to have a size factor of 1.5, with 5.3% savings in annual HVAC energy use. Similarly, design only optimization results in 4.4% savings in annual HVAC energy demand. Combined design and control optimization not only yields a higher energy savings compared to each of the individual optimization options, but it also does not require any pre-determined selection of either design specifications or control settings.

4. Sensitivity Analysis

The previous section describes the potential benefits of optimizing simultaneously the design and control of the heat pump for specific set of conditions including climate, performance curve, compressor type, and airflow rate. This section performs a series of sensitivity analyses to assess the impacts of various heat pump system parameters and operating conditions on the benefits of combined design and control of heat pumps.

4.1 Effect of varying airflow rate

Previously the design optimization problem was set up by changing only the capacity of the heat pump while keeping the airflow rate constant. In this section, the airflow rate passing through the heat pump is also included as a variable parameter in the design optimization. Typically, both the airflow rate and the heating/cooling capacity are interdependent. Indeed, the heating and cooling capacities delivered by a heat pump is directly correlated to the delivered air flow rate. In this study, a different sizing factor than that used for heating/cooling capacity is considered for the airflow rate to allow options for the heat pump to operate at variable air flow rates. Specifically, the airflow rate is set to vary from 0.8 to 2 times the value set for the adjusted baseline.

The combined design and control optimization results, illustrated in Figure 8, indicate that there is no significant difference in energy savings obtained by changing the airflow rate and those achieved when setting this rate constant. Although maintaining the flow rate constant at the baseline value would restrict the range of feasible heating/cooling capacities for the heat pump, the level of energy savings that could be achieved from the combined design and control remain practically unchanged.

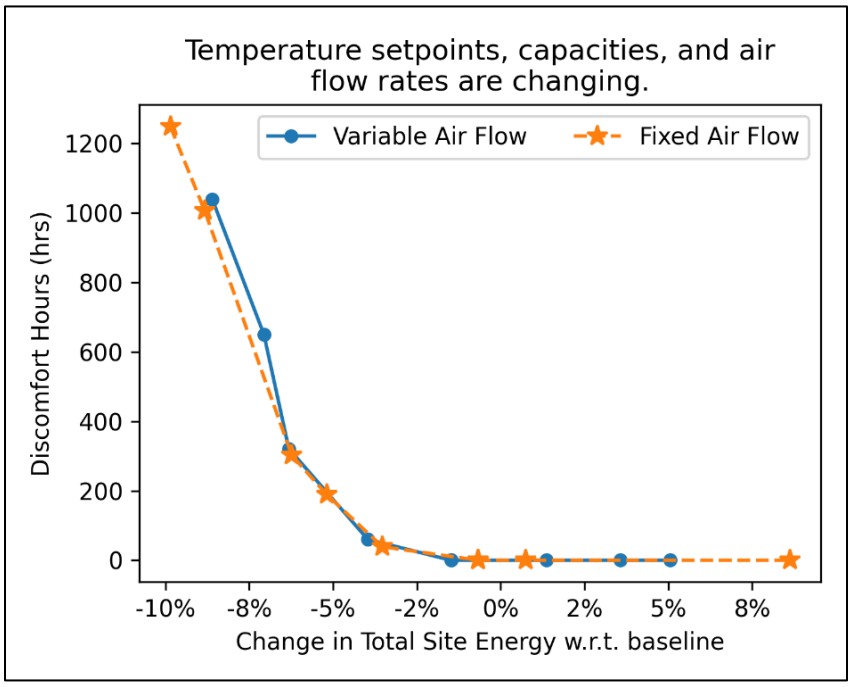

Figure 8 Pareto fronts of solutions obtained by optimizing both design and control settings for variable and constant airflow rates

4.2. Effect of heat pump performance curve

The performance of heat pumps depends on several factors including airflow rate as noted in the previous section as well as inlet and outlet air temperatures. Heat pumps are described by their performance at standard rating conditions as specified by AHRI [22] and a set of performance curves at other operating conditions. These performance curves, modeled by EnergyPlus, describe the capacity and energy efficiency of the heat pump as a function of air temperature entering the evaporator and the condenser and the airflow rate.

1. *Capacity performance curves*
   The fraction of the actual to rated cooling capacities can be expressed as a polynomial function:

$$\frac{\dot{Q}_c}{\dot{Q}_{r,c}} = f_C^T\left(T_{wb,in}^e, T_{db,in}^c\right) f_C^V\left(\frac{\dot{V}}{\dot{V}_r}\right) \tag{7}$$

   Where $\dot{Q}_c$ is the actual cooling capacity, $\dot{Q}_{r,c}$ is the cooling capacity at rated conditions, $T_{wb,in}^e$ is the wetbulb temperature of the air entering the evaporator (i.e., indoor unit of the heat pump) and $T_{db,in}^c$ is the dry bulb temperature of air entering the condenser (i.e., outdoor unit of the heat pump), $\left(\frac{\dot{V}}{\dot{V}_r}\right)$ which is the ratio of actual airflow rate relative to rated airflow rate and f_C^T and f_C^V biquadratic and quadratic polynomial functions respectively. A similar capacity performance curve is defined for heating.

2. *Energy efficiency performance curves*
   The energy efficiency of a heat pump is expressed using the Energy Input Ratio (EIR) defined as the inverse of the Coefficient of Performance (COP). Like the capacity, energy efficiency is also expressed as ratio of the actual EIR over the EIR at rated conditions which is a function of condenser and evaporator temperatures and ratio of actual to rated airflow rates:

$$\frac{EIR}{EIR_r} = f_{EIR}^T\left(T_{wb,in}^e, T_{db,in}^c\right) f_{EIR}^V\left(\frac{\dot{V}}{\dot{V}_r}\right) \tag{8}$$

   Where f_{EIR}^T is a biquadratic function while f_{EIR}^V is a quadratic function.

Therefore, the power used by the heat pump can be determined by multiplying the actual capacity delivered by the actual EIR. However, due to cycling of the heat pump during its operation some losses could occur which can be accounted for using a correction factor called the Run Time Fraction (RTF) as indicated by Eq. (9) and Eq. (10):

$$\dot{P} = EIR\ x\ \dot{Q}_C\ x\ RTF \tag{9}$$

Where,

$$RTF = \frac{PLR}{PLF} \tag{10}$$

PLR is the part load ratio of the compressor defined as the ratio of the actual sensible load to the rated sensible capacity delivered by the coil, and PLF is the part load fraction which is expressed a function of the PLR:

$$PLF = C_1 + C_2(PLR) + C_3(PLR)^2 \quad (11)$$

Cutler et al [28] conducted a series of sensitivity analyses to determine the impact on energy demand for heating and cooling of performance curves obtained from five different manufacturers of single speed residential heat pumps. They found that changes in performance curves do not have a significant impact on annual energy use of the heat pump. They also recommended a set of standard performance curves for heat pump systems. Figure 9 compares the standard curves described in their study against those used in this study for the original baseline case. In this section, performance curves from Cutler at al. [28] are used to assess their impacts on the combined design and control optimization results as summarized in Figure 9.

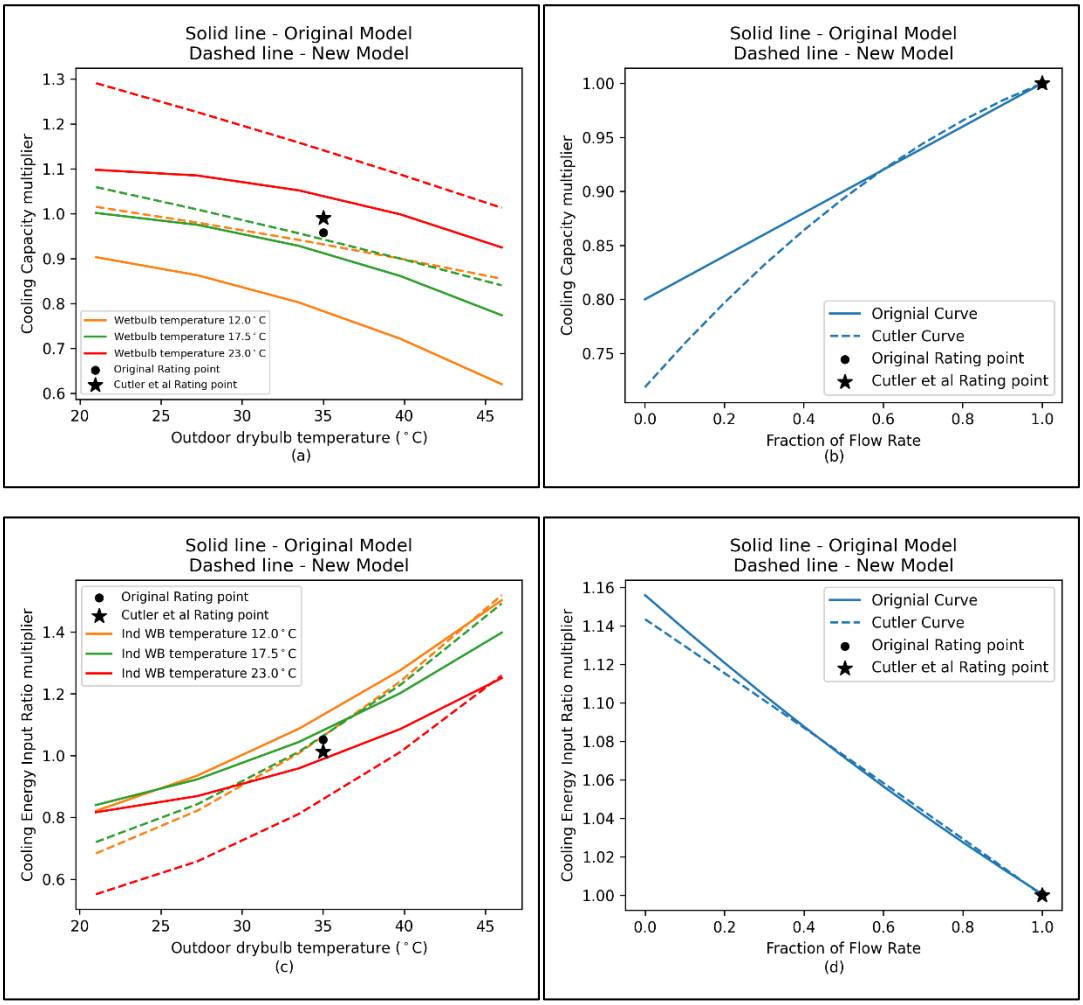

Figure 9 Comparison of prototypical cooling coil performance curves obtained from Cutler et al [28] with the curves from the original system provided in the DOE residential building energy model where the cooling capacity and Energy Input Ratio multipliers are shown as functions of (a),(c) outdoor dry-bulb and indoor wet bulb temperature, and (b),(d) fraction of air flow rate.

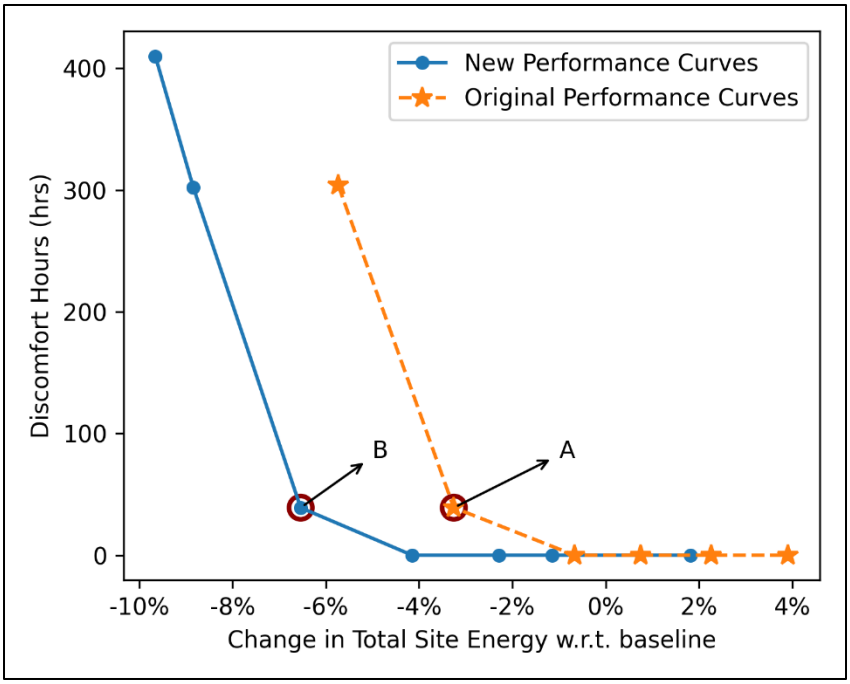

Figure 10 Pareto fronts solutions obtained by optimizing both design and control settings for two different performance curves of the heat pump.

Table 8 Specifications and performance indicators for optimal solutions with two different performance curves

Index	Main Coil Sizing Factor	Supplementary Coil sizing factor	Heating Setpoint	Cooling Setpoint	Reduction in total site energy w.r.t. baseline	Reduction in HVAC energy use w.r.t. baseline	Discomfort Hours
A	1.95	1.55	$23.0°C$	$26.0°C$	-6.5%	-13.8%	39
B	1.80	1.50	$23.0°C$	$26.0°C$	-3.25%	-7.2%	39

Figure 10 compares the Pareto fronts obtained from the combined design and control optimization results using two different performance curves of the heat pump. Table 8 lists the specifications and performance metrics including annual site energy use and thermal discomfort hours for optimal solutions correspondent to the different heat pump performance curves. The results of Figure 9 and Table 10 indicate that the standard performance curves from Cutler et al [28] yield higher energy savings for the same number

of thermal discomfort hours compared to those achieved for the original performance curves. Indeed, the energy savings are doubled even though the design and the control parameters have not changed significantly when different performance curves are considered for the heat pump. These results demonstrate that it is crucial to use the appropriate performance curves for the heat pump system before selecting its optimal design specifications and control settings as these curves can affect significantly both annual energy needs and thermal comfort levels.

4.3 Effect of compressor type

In this section, the impacts of using variable speed compressor are assessed when combining design and control optimization for the heat pump. Generally, variable speed compressors consume less energy than single speed systems due to their higher efficiency at part load conditions. In this section, a 4-speed compressor is considered for the heat pump. Following the EnergyPlus modeling approach, rated capacities, airflow rates, COP values, and performance curves for each speed are defined for both heating and cooling operations [22]. Table 9 compares the capacities and COP values of the single speed and four-speed heat pump configurations considered in this analysis.

Table 9 Comparison of the specifications of the single speed and multispeed system.

Type of System	**Main Coil Size**	**Supplementary Coil size**	**COP in cooling**	**COP in heating**
Single Speed	5.75 kW (19630 Btu/hr)	6.48 kW (22117 Btu/hr)	4.07	3.69
Multi Speed	5.75 kW (100%)	6.48 kW	4.07	3.69
	4.6 kW (80%)	6.48 kW	5.00	4.20
	4.02 kW (70%)	6.48 kW	6.00	5.00
	3.45 kW (60%)	6.48 kW	6.50	5.50

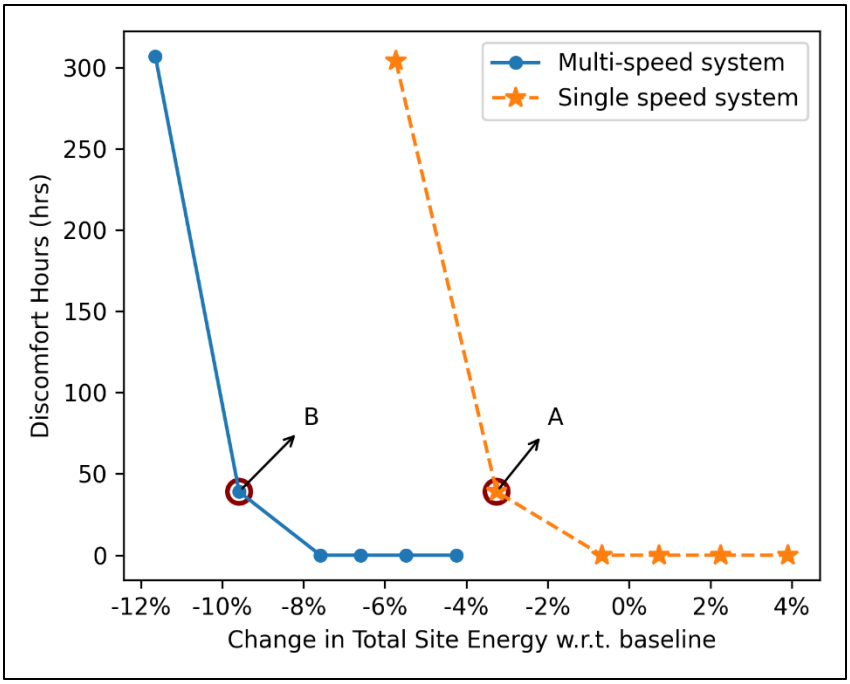

Figure 11 Pareto fronts of solutions obtained by optimizing both design and control parameters for single and multiple speed heat pumps.

Table 10 Specifications and performance metrics for optimal solutions specific to single and multiple speed heat pumps

Type of System	**Main Coil Sizing Factor**	**Supplementary Coil sizing factor**	**Heating Setpoint**	**Cooling Setpoint**	**Reduction in total site energy w.r.t. baseline**	**Reduction in HVAC energy use w.r.t. baseline**	**Discomfort Hours**
Single Speed	1.8	1.5	$23.0°C$	$26.0°C$	-3.3%	-7.2%	39
Multispeed system (4 speeds)	2.0	1.7	$23.0°C$	$26.0°C$	-9.6%	-21.2%	39

Figure 11 show Pareto fronts obtained from combined design and control optimization using the single speed and the 4-speed heat pump. Table 12 summarizes the design and control specifications as well as performance metrics of two specific optimal solutions outlined in Figure 10. As expected and due to its

higher energy efficiency, the multiple speed heat pump provides significant energy savings relative to the adjusted baseline case resulting in tripling the reduction in total site energy use compared to the optimal solution obtained from the single speed heat pump. While the multi-speed heat pump requires the same optimal temperature setpoints as the single speed heat pump, its optimal capacities are higher for both the main and supplementary coils.

4.4. Effect of the climatic conditions

In this analysis, the impact of the climate is investigated by considering two other US cities located in different climatic zones for the prototypical house in addition to Boulder, CO, including Phoenix, AZ, and San Francisco, CA. Table 11 compares the main climatic characteristics of the three US locations considered in this section including their ASHRAE climate zone, heating degree-days (HDD), cooling degree-days (CDD), and average daily solar radiation [29].

Table 11 Features of the three climate regions considered in the analysis.

City	Longitude	ASHRAE Climate Zone	Climate Characteristics	HDD18.3 ($°C - days$)	CDD18.3 ($°C - days$)	Average daily solar radiation ($\frac{kWh}{m^2}\ per\ day$)
Phoenix, AZ	$-122.839°$	2B	Hot-Dry	486	2610	5.8
San Francisco, CA	$-122.839°$	3C	Marine	1448	96	4.9
Boulder, CO	$-105.217°$	5B	Cold	2968	478	4.6

4.4.1. Phoenix, AZ

Phoenix, AZ, is part of the ASHRAE climate zone 2B which is categorized with hot and dry weather conditions. The prototypical residential building model specific to the climate zone 2B from [20] is used along with the baseline heat pump specifications summarized in Table 12.

Table 12: Heating and Cooling Capacities for the Prototypical Air Source Heat Pump in climate zone 2B.

	Coil Type	Supply Air Flow Rate [m^3/s]	COP	Nominal Capacity [kW]
Cooling	Single Speed DX cooling coil	0.414	4.068	7.58
Heating	Single Speed DX heating coil	0.414	3.69	7.58
Supplementary heating	Electric heating coil	0.414	–	4.58

Three optimization studies are carried out to assess the benefits of combined design and control optimization over individual optimizations (i.e., design only and control only) for this climate using coil

capacity and temperature setpoints as the design and control variables, respectively. Figure 12 shows the Pareto curves obtained for each of the three optimization cases.

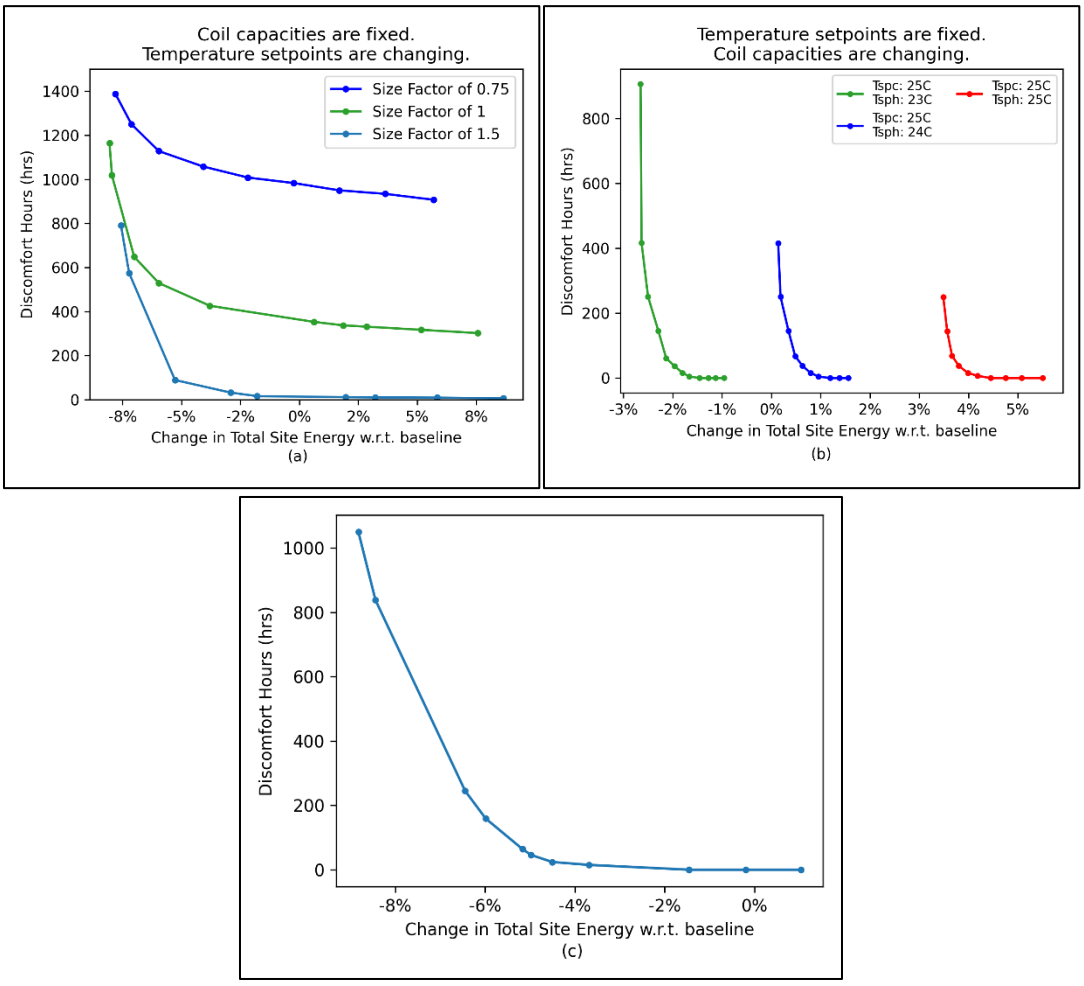

Figure 12 Pareto curves for the bi-objective optimization of energy consumption and thermal discomfort for (a) control only optimization, (b) design only optimization and, (c) combined design and control optimization.

Specifically, Figure 12 indicates the variation of thermal discomfort hours against the reduction in annual total energy consumed by the house site relative to the adjusted baseline case. Table 13 summarizes the best optimal design and control parameters for each of the three optimization studies with similar levels of thermal discomfort.

Table 13 Comparison of system specifications and performance indicators for the three optimization case studies with similar level of thermal discomfort.

	Main Coil Size		**Supplementary Coil Size**		**Heating Setpoint**		**Cooling Setpoint**		**Reduction in Total Site Energy w.r.t. baseline**	**Reduction in HVAC energy use w.r.t. baseline**	**Discomfort Hours**
	Base	Opt	Base	Opt	Base	Opt	Base	Opt			

Control Only	1.8	1.5	0.9	1.5	$23.5°C$	$22.5°C$	$25°C$	$25°C$	-2.9%	-8.3%	32
Design Only	1.8	1.4	0.9	1.4	$23.5°C$	$23°C$	$25°C$	$25°C$	-1.9%	-6.8%	37
Combined Design and Control	1.8	1.7	0.9	1.5	$23.5°C$	$22.5°C$	$25°C$	$25.5°C$	-4.9%	-11.8%	46

For similar number of thermal discomfort hours, the best solution with control only optimization yielded 8.3% savings in HVAC annual energy end-use while design only optimization results in a 6.8% reduction. However, the combined design and control optimization led to higher energy savings with a 11.8% reduction in HVAC energy consumption. These energy reductions obtained in Phoenix, AZ, indicate that the benefits of combined design and control optimization are higher for hot climates than those achieved for Boulder, CO, characterized as a cold climate.

4.4.2. San Francisco, CA

San Francisco, CA, belongs to the ASHRAE climate zone of 3C and is characterized with warm and marine climatic conditions [29]. The baseline heat pump specifications for the climate zone 3C are listed in Table 14.

Table 14: Heating and Cooling Capacities for the Prototypical Air Source Heat Pump in climate zone 3C.

	Coil Type	**Supply Air Flow Rate [m^3/s]**	**COP**	**Nominal Capacity [kW]**
Cooling	Single Speed DX cooling coil	0.248	4.068	4.42
Heating	Single Speed DX heating coil	0.248	3.69	2.83
Supplementary heating	Electric heating coil	0.248	–	2.83

The results from optimization studies conducted when the prototypical residential building is in San Francisco are shown in Figure 13 and summarized in Table 15.

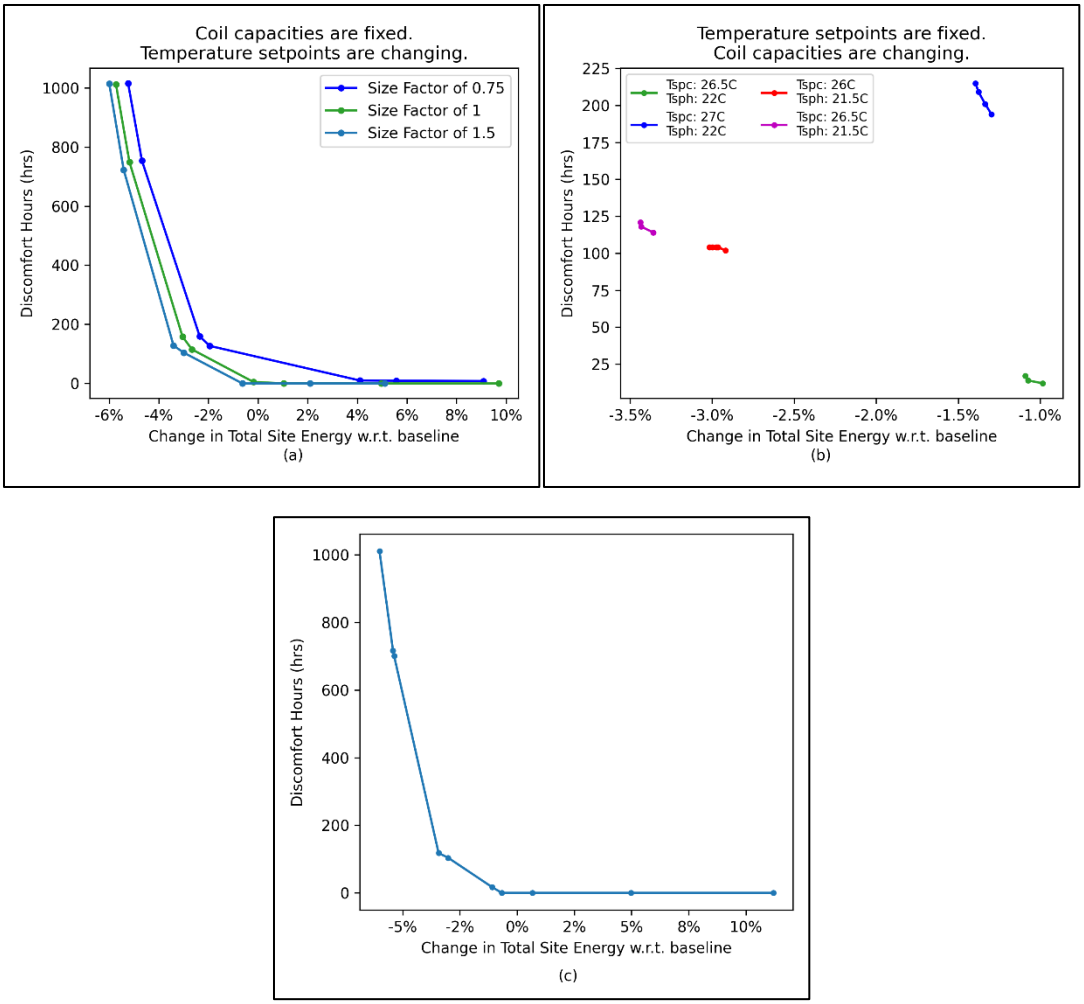

Figure 13 Pareto curves for the bi-objective optimization of energy consumption and thermal discomfort for (a) control only optimization, (b) design only optimization and, (c) combined design and control optimization.

Table 15 Comparison of system specifications and performance indicators for the three optimization studies with total number of discomfort hours less than 300.

	Main Coil Size		**Supplementary Coil Size**		**Heating Setpoint**		**Cooling Setpoint**		**Reduction in Total Site Energy w.r.t. baseline**	**Reduction in HVAC energy use w.r.t. baseline**	**Discomfort Hours**
	Baseline	Optimal	Baseline	Optimal	Baseline	Optimal	Baseline	Optimal			
Control Only	1.9	1.5	0.9	1.5	$22°C$	$21.5°C$	$25.5°C$	$25.5°C$	-2.44%	-16%	104

Design Only Optimization	1.9	2.0	0.9	1.7	$22°C$	$22°C$	$25.5°C$	$27°C$	-1.3%	-6.92%	194
Combined Design and Control	1.9	1.7	0.9	0.9	$22°C$	$21.5°C$	$25.5°C$	$26°C$	-3.0%	-18.3%	104

For the mild climate of San Francisco, CA, the annual energy consumed by HVAC equipment for is lower than the energy consumed by other end uses including lighting and appliances. As shown in Figure 13 and summarized in Table 15, the best case of design only optimization yielded a 7% reduction in HVAC annual energy end-use along with an increase in the number of thermal discomfort hours whereas control only optimization reduced the HVAC energy end-use by 16%. In contrast, the combined design and control optimization achieves 18% savings in annual HVAC energy end-use. These energy reductions obtained in San Francisco, CO, are higher than those achieved for both Boulder, CO, and Phoenix, AZ. Indeed, San Francisco, CA, is characterized by a mild climate and offers a balanced operation between heating and cooling modes for the heat pump.

5. Summary and Conclusions

This study has investigated the benefits of a new analysis approach to simultaneously optimize both the combining design specifications and control settings of heat pumps to maximize both energy efficiency and indoor thermal comfort specific to residential buildings. First, the baseline design and control parameters are adjusted to ensure that indoor thermal comfort is achieved throughout the year for a prototypical US residential building. Then, individual as well as combined design and control optimization analyses are performed to minimize both the annual energy consumption and the number of thermal discomfort hours. The hourly thermal discomfort is determined by estimating the Predicted Mean Vote (PMV) using whole-building energy simulation analysis.

The results of the analysis indicate that 3.3% of total energy consumption and 7.2% of HVAC energy end-use can be saved annually when integrating design and control optimization relative to a baseline case adjusted to achieve acceptable indoor thermal comfort throughout the year. Moreover, it is found that design only and control only optimizations yield respectively, 4.4% and 5.3% reduction in HVAC annual energy use compared to the adjusted baseline case. In addition to higher energy savings, the combined design and control optimization can inform during the early design phase on the best operating strategies to maximize the indoor thermal comfort levels without the need to make any pre-determined assumption about the control settings.

Through a series of sensitivity analyses, it is found that that the energy savings achieved by the combined design and control optimization depend significantly on various heat pump characteristics including compressor types, coil performance curves, and climate features. For instance, the use of multi-speed compressor can triple the savings associated with HVAC annual energy end use when the design and control optimization is combined. The magnitude of potential energy savings obtained from the combined design and control optimization is found to depend on the climatic conditions with higher energy savings achieved in locations with hot and especially mild climates.

In general, integrating the optimization of both the design and the control parameters is highly recommended when specifying heat pump systems. Indeed, the combined design and control optimization can provide significant benefits compared to only optimizing the design parameters of heat pumps as is the case of current practices when electrifying buildings. However, the integrated design and control optimization, like the design only optimization, requires detailed prior knowledge of the characteristics of the considered heat pumps including their compressor type and performance curves.

One main limitation of the analysis performed in this study is the use of a deterministic analysis which does not account for real-time variations in building operating conditions and energy prices. Therefore, actual savings in real buildings might differ from those estimated in this study due to potential variations in operations conditions. Further investigation of the benefits of combined design and control optimization coupled with predictive controls is necessary to better account for real heat pump operation conditions. However, the potential savings achieved by the combined design and control optimization of the heat pump indicate that higher benefits could be obtained when integrated with other energy systems such domestic hot water systems, appliances, and PV systems during the early design stages of electrifying buildings. Future work should consider evaluating the additional benefits of combined design and control optimization when integrating various energy systems as part of assessing the best electrification strategies of new and existing buildings.

Declaration of competing interest: The authors declare that they have no competing interests that could have influenced the results of this paper.

Acknowledgements: The funding for this study by the BEST Center established, under NSF grants No. 213874 and No. 2113907, is acknowledged. Moreover, the guidance throughout the execution of the study from Mr. Chris Day, Rheem, David Podorson, Xcel Energy, and Brent Constant, Mitsubishi Electric Trane, is highly appreciated.

References

[1] EIA, "Residential Energy Consumption Survey (RECS), Energy Information Administration . Washington, DC.," 2020.

[2] "Energy Consumption by Sector and Source, Annual Energy Outlook 2023, https://www.eia.gov/outlooks/aeo/."

[3] K. A. Barber and M. Krarti, "A review of optimization based tools for design and control of building energy systems," *Renew. Sustain. Energy Rev.*, vol. 160, p. 112359, May 2022, doi: 10.1016/j.rser.2022.112359.

[4] D. Patteeuw and L. Helsen, "Combined design and control optimization of residential heating systems in a smart-grid context," *Energy Build.*, vol. 133, pp. 640–657, Dec. 2016, doi: 10.1016/j.enbuild.2016.09.030.

[5] R. Evins, "Multi-level optimization of building design, energy system sizing and operation," *Energy*, vol. 90, pp. 1775–1789, Oct. 2015, doi: 10.1016/j.energy.2015.07.007.

[6] D. B. Crawley, L. K. Lawrie, C. O. Pedersen, and F. C. Winkelmann, "Energy plus: energy simulation program," *ASHRAE J.*, vol. 42, no. 4, pp. 49–56, 2000.

[7] Klein, S.A., et al., "TRNSYS, A Transient Simulation Program. Version 17, University of Wisconsin-Madison, Madison, WI." 2018.

[8] T. Nouidui, M. Wetter, and W. Zuo, "Functional mock-up unit for co-simulation import in EnergyPlus," *J. Build. Perform. Simul.*, vol. 7, no. 3, pp. 192–202, May 2014, doi: 10.1080/19401493.2013.808265.
[9] "Spawn of Energy Plus, http://lbl-srg.github.io/soep/."
[10] M. Wetter, P. Haves, and B. Coffey, "Building Controls Virtual Test Bed," Lawrence Berkeley National Laboratory (LBNL), Berkeley, CA (United States), BCVTB, Apr. 2008. doi: 10.11578/dc.20210416.27.
[11] H. Bahlawan, M. Morini, M. Pinelli, P. R. Spina, and M. Venturini, "Simultaneous optimization of the design and operation of multi-generation energy systems based on life cycle energy and economic assessment," *Energy Convers. Manag.*, vol. 249, p. 114883, Dec. 2021, doi: 10.1016/j.enconman.2021.114883.
[12] A. Ashouri, S. S. Fux, M. J. Benz, and L. Guzzella, "Optimal design and operation of building services using mixed-integer linear programming techniques," *Energy*, vol. 59, pp. 365–376, Sep. 2013, doi: 10.1016/j.energy.2013.06.053.
[13] L. Urbanucci, F. D'Ettorre, and D. Testi, "A Comprehensive Methodology for the Integrated Optimal Sizing and Operation of Cogeneration Systems with Thermal Energy Storage," *Energies*, vol. 12, no. 5, Art. no. 5, Jan. 2019, doi: 10.3390/en12050875.
[14] F. Ascione, N. Bianco, C. De Stasio, G. M. Mauro, and G. P. Vanoli, "A new comprehensive approach for cost-optimal building design integrated with the multi-objective model predictive control of HVAC systems," *Sustain. Cities Soc.*, vol. 31, pp. 136–150, May 2017, doi: 10.1016/j.scs.2017.02.010.
[15] K. Deb, A. Pratap, S. Agarwal, and T. Meyarivan, "A fast and elitist multiobjective genetic algorithm: NSGA-II," *IEEE Trans. Evol. Comput.*, vol. 6, no. 2, pp. 182–197, Apr. 2002, doi: 10.1109/4235.996017.
[16] S. Fazlollahi, P. Mandel, G. Becker, and F. Maréchal, "Methods for multi-objective investment and operating optimization of complex energy systems," *Energy*, vol. 45, no. 1, pp. 12–22, Sep. 2012, doi: 10.1016/j.energy.2012.02.046.
[17] T. Beck, H. Kondziella, G. Huard, and T. Bruckner, "Optimal operation, configuration and sizing of generation and storage technologies for residential heat pump systems in the spotlight of self-consumption of photovoltaic electricity," *Appl. Energy*, vol. 188, pp. 604–619, Feb. 2017, doi: 10.1016/j.apenergy.2016.12.041.
[18] J. D. Fonseca, J.-M. Commenge, M. Camargo, L. Falk, and I. D. Gil, "Multi-criteria optimization for the design and operation of distributed energy systems considering sustainability dimensions," *Energy*, vol. 214, p. 118989, Jan. 2021, doi: 10.1016/j.energy.2020.118989.
[19] E. D. Mehleri, H. Sarimveis, N. C. Markatos, and L. G. Papageorgiou, "Optimal design and operation of distributed energy systems: Application to Greek residential sector," *Renew. Energy*, vol. 51, pp. 331–342, Mar. 2013, doi: 10.1016/j.renene.2012.09.009.
[20] Dept. of Energy, "Prototypical Residential Building Models, DOE, https://www.energycodes.gov/prototype-building-models#Residential."
[21] E. Wilson, C. Engebrecht-Metzger, S. Horowitz, and R. Hendron, "2014 Building America House Simulation Protocols," National Renewable Energy Lab. (NREL), Golden, CO (United States), NREL/TP-5500-60988, Mar. 2014. doi: 10.2172/1126820.
[22] U.S. DOE, *Energy Plus Engineering Reference, Version 22.2.0*. 2022.
[23] ANSI/ASHRAE/IES, *ANSI/ASHRAE/IES 55-2020, Thermal Environmental Conditions for Human Occupancy. American Society of Heating, Refrigerating and Air-Conditioning Engineers, Atlanta, Georgia.*
[24] Y. Zhang, "JEA, An Interactive Optimisation Engine for Building Energy Performance Simulation," presented at the Building Simulation 2017, in Building Simulation, vol. 15. IBPSA, 2017, pp. 2232–2241. doi: 10.26868/25222708.2017.607.
[25] B.V. Mbuwir, D. Geysen, G. Kosmadakis, M. Pilou, G. Meramveliotakis, H. Toersche, "Optimal control of a heat pump-based energy system for space heating and hot water provision in buildings:

Results from a field test", Energy and Buildings, 310,114116, 2024. https://doi.org/10.1016/j.enbuild.2024.114116.
[26] M. Dongellini, C. Naldi, G.L. Morini, "Influence of sizing strategy and control rules on the energy saving potential of heat pump hybrid systems in a residential building", Energy Conversion and Management, 235,114022, May 2021. https://doi.org/10.1016/j.enconman.2021.114022.
[27] F. Chiu, and M. Krarti, "Impacts of Air-Conditioning Sizing on Energy Performance of US Office Buildings", ASME Journal of Engineering for Sustainable Buildings and Cities, 2(2), 021001-1-14, May 2021. https://doi.org/10.1115/1.4050937.
[28] D. Cutler, J. Winkler, N. Kruis, C. Christensen, and M. Brendemuehl, "Improved Modeling of Residential Air Conditioners and Heat Pumps for Energy Calculations," National Renewable Energy Lab. (NREL), Golden, CO (United States), NREL/TP-5500-56354, Jan. 2013. doi: 10.2172/1067909.
[29] American Society of Heating, Refrigerating and Air-Conditioning Engineers., *2021 ASHRAE Handbook Fundamentals (SI Edition)*. American Society of Heating Refrigerating and Air-Conditioning Engineers Inc.